Chapter 1

INTRODUCTION

1.1. MOTIVATION AND BACKGROUND

1.1.1. Research with femtosecond laser pulses

Understanding the propagation of femtosecond light pulses is of great value for both scientific and technological applications. The short pulse duration provides scientists with the possibility to explore physical phenomena with unprecedented time resolution; chemical reactions can be studied at the atomic level, and ultrafast changes in material properties can be measured. The high intensity levels achieved with ultrashort laser pulses create strong nonlinear light-matter interactions, which have led to new optical phenomena, such as the formation of spatio-temporal solitons [1,2] and the generation of coherent white light (white light laser [3]). Solitons are “solitary waves” that can propagate for a long distance with a constant shape and can interact with other solitons. The formation and propagation of solitons is of great interest for applications in optical communications and optical computing.

The advent of commercially available femtosecond lasers has triggered a wealth of new technologies, such as micromachining with femtosecond pulses, multiphoton imaging techniques and femtosecond LIDAR (Light detection and ranging). There have also been improvements to existing technologies, such as the use of femtosecond lasers in corrective eye surgery and Optical Coherence Tomography. There have also been many advances in the characterization and manipulation of pulses. Single-shot autocorrelators and spectrum analyzers can be replaced by frequency resolved optical gating (FROG [4]) devices that capture a more complete description of the pulse properties. The pulses can be manipulated and transformed for specific applications using either grating based pulse-shapers, photonic crystal fibers, optical amplifiers, crystals for harmonic generation, etc. The widespread use of femtosecond lasers by researchers across different fields suggests even more applications are on the way. In many cases the interaction of the pulses with matter is very complex due to the strong nonlinear effects and is still not fully understood. I hope that the work presented here will shed some light on this very interesting problem.

1.1.2. Ultrafast cameras

The need to image fast phenomena has lead to many novel technologies and ever-faster imaging systems. Film-based cameras capture events in microseconds by using mechanical motion to direct the light to different parts of the film. Digital cameras with electro-optic switches can reach nanosecond frame rates. The speed of the electronics limits these cameras from achieving speeds much below a nanosecond [5]. Streak cameras can operate at picosecond or even sub-picosecond resolution, but provide only 1-dimensional information [6]. Holographic methods have also been implemented to observe fast events. The most common holographic technique for fast recording is double exposure interferometry, but is limited to only two frames. Light in flight recording [7] can capture the propagation of picosecond pulses through optical elements. However, this technique captures the scattering of the beam from a rough surface and cannot capture the beam profile inside the medium. More recently, a holographic camera was developed to capture events with nanosecond frame rates [8,9]. Nanosecond resolution can be used to observe fast phenomena like plasma formation and the evolution of shock waves. In order to observe the propagation of light pulses, however, we need to push the temporal resolution to sub-picosecond.

We have developed a holographic imaging system that captures nonlinear pulse propagation with 150-femtosecond time resolution and recovers amplitude and phase information. The propagation is captured using digital on-axis holography [10] and spatial multiplexing. The holograms are recorded on a CCD camera and reconstructed numerically. On-axis holograms do not require separate signal and reference pulses; both the signal and reference are generated by a single probe pulse. The use of self-referenced holograms allowed us to capture a time-sequence of the event by spatially separating four holograms on a single frame of the CCD camera. The holographic system records either a single hologram with high spatial resolution (4 µm) or a time-sequence of four holograms (holographic movie) with reduced spatial resolution. Holography allows us to recover amplitude and phase information and to record a time-sequence of holograms in a single shot experiment. Nonlinear index changes in the material can be recovered from the phase information. Positive index changes are in general due to the Kerr nonlinearity, while negative index changes can appear if the intensity of the laser pulses reaches the ionization threshold. Plasma generation induces a negative index change that is proportional to the density of free electrons.

1.1.3. Visualization of the propagation of femtosecond pulses

Several methods have been implemented to visualize the propagation of femtosecond pulses. If temporal resolution is not required, one can measure a trace left in a material after a pulse has gone through and reconstruct the time-integrated spatial profile of the beam. For example, for pulse propagation through solids, if there is permanent damage in the material the beam profile can be inferred from the damage tracks. In the case of fluids, the trace can be visualized by dissolving a fluorescent dye in the material and capturing a side view of the fluorescence [11] or by imaging the light emission from plasma generated by the pulse.

Pump-probe experiments can capture the time evolution if the event is repeatable. Care must be taken to ensure the experimental conditions do not change during the experiment. A pump pulse is used to generate the ultrafast event, and a probe with a variable time delay is used to observe it as a function of time. The time evolution of the event can be recovered by combining multiple experiments with different time delays. A probe pulse can monitor the reflectivity or transmission of a sample directly. An alternative to holography for measuring the nonlinear index change due to the Kerr effect is Femtosecond Time-resolved

Optical Polarigrahpy (FTOP) [12]. This technique monitors changes in the polarization of the probe that result from birefringence induced in medium. We have used this technique to study the behavior of spatial solitons in 1-D arrays (Chapter 5, [13]). The advantage of FTOP is that it has a high sensitivity, while the drawback is that it can only capture birefringence and not isotropic index changes such as the plasma index change.

The pulse propagation can also be studied by directly measuring the beam profile as a function of energy and propagation length. Increasing the pulse energy causes the beam to self-focus and break up in a shorter distance. Varying the energy and propagation distance allowed us to do a comprehensive study of pulse propagation through a nonlinear liquid (Chapter 4, [14]). The propagation distance was adjusted by changing the height of the liquid in-situ. Combining the results obtained with the holographic system, the propagation as a function of energy and length, and the results with FTOP, we were able to investigate the process of beam breakup, the formation of spatial solitons and their interactions, and the collective behavior of the solitons that results from interactions.

1.2. LASER SYSTEM AND DIAGNOSTICS

In our experiments we have used femtosecond pulses from a Titanium:Sapphire laser amplifier system (Fig. 1.1). The amplifier requires a seed laser, which provides low energy femtosecond pulses, and a pump laser. The seed laser is a Ti:Sapphire femtosecond laser (Coherent Mira 900), which provides 100-200 femtosecond pulses at a wavelength of 800 nm (tunable from 700-900 nm) with a repetition rate of 76 MHz and average power up to 1 W. The laser uses a passive Kerr-lens modelocking system and intra-cavity dispersion compensation prisms. The Mira is pumped by a CW multi-line argon laser (Coherent Innova 300C) with a power of 8 W. The seed pulses are fed into a Spectra Physics TSA regenerative amplifier. The TSA is pumped by a frequency doubled Nd:Yag laser (Spectra Physics Quanta Ray Lab 150), which generates 6-nanosecond pulses with a repetition rate of 10 Hz, and maximum energy of 300 mJ at a wavelength of 532 nm. The seed pulses are stretched in the TSA using a grating pair and inserted into a cavity with a Ti:Sapphire crystal. Pump pulses with 50-mJ energy are synchronized with the seed pulses and inserted in the cavity. After multiple passes through the Ti:Sapphire crystal the femtosecond pulses are switched out of the cavity and recompressed with the grating pair. The pulses are switched in and out of the cavity using Pockels cells. The output pulses have a maximum energy of 2 mJ, 150-femtosecond pulse duration, wavelength of 800 nm and repetition rate of 10 Hz.

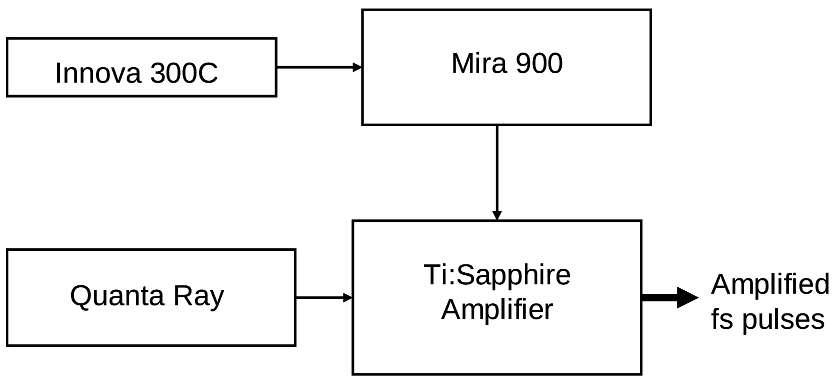

Figure 1.1. Schematic diagram of the laser system. A seed femtosecond laser (Mira 900) and a pump nanosecond laser (Quanta Ray) are used to feed the amplifier (TSA). The Mira is pumped by a CW argon ion laser (Innova 300C).

A frequency-resolved optical gating (FROG) device is used to characterize the output pulses from the Mira and the TSA. The technique can measure the intensity and phase of the pulses as a function of time. The device is a Grenouille from Swamp Optics, which can measure pulses from 30-300 femtoseconds. The FROG traces are processed in real time using the VideoFrog software package from Southwest Science. Figure 1.2 shows a screen capture of the trace and the reconstruction of typical output pulses from the Mira (seed laser). After the amplification there is some distortion of the pulses. Figure 1.3 shows a screen capture of the output pulses from the TSA. The amplified pulses are measured in a single-shot, while the measurement of the seed pulses is averaged over many pulses.

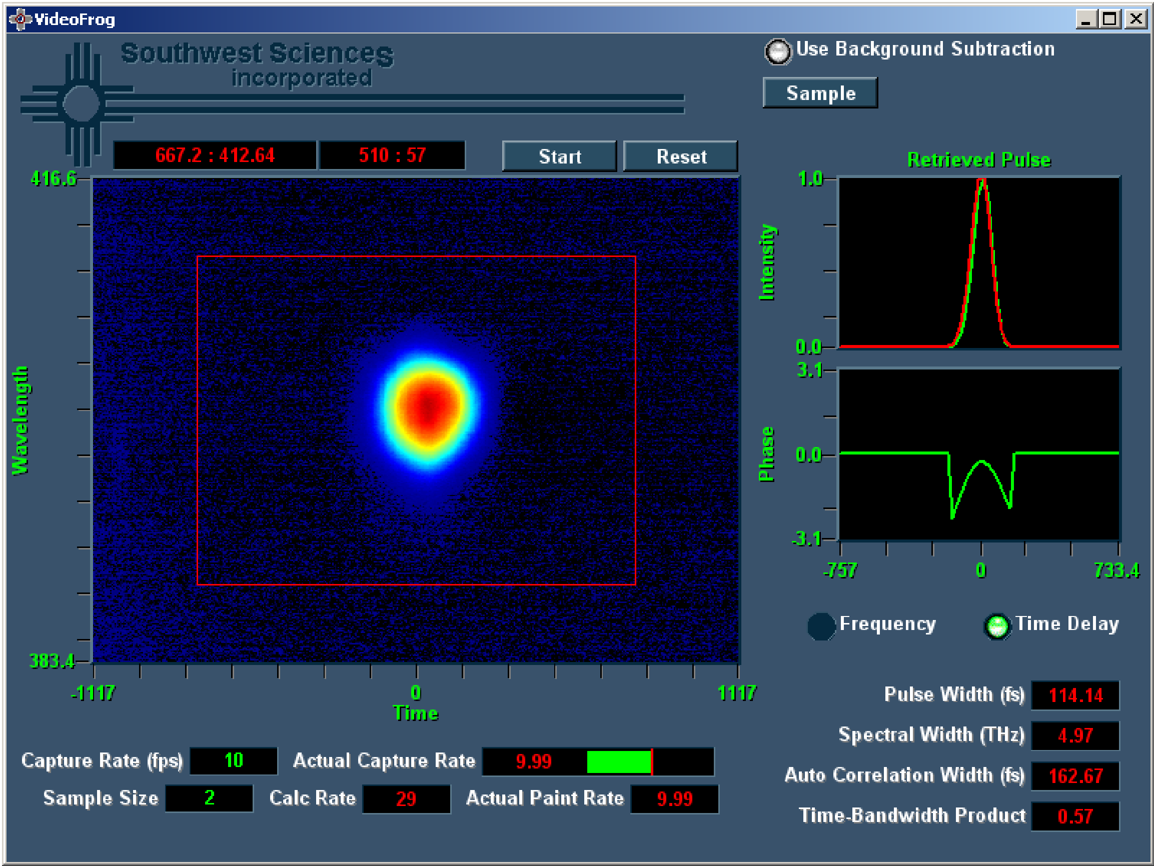

Figure 1.2. Screen capture of the FROG trace and reconstruction of pulses from the seed laser (Mira).

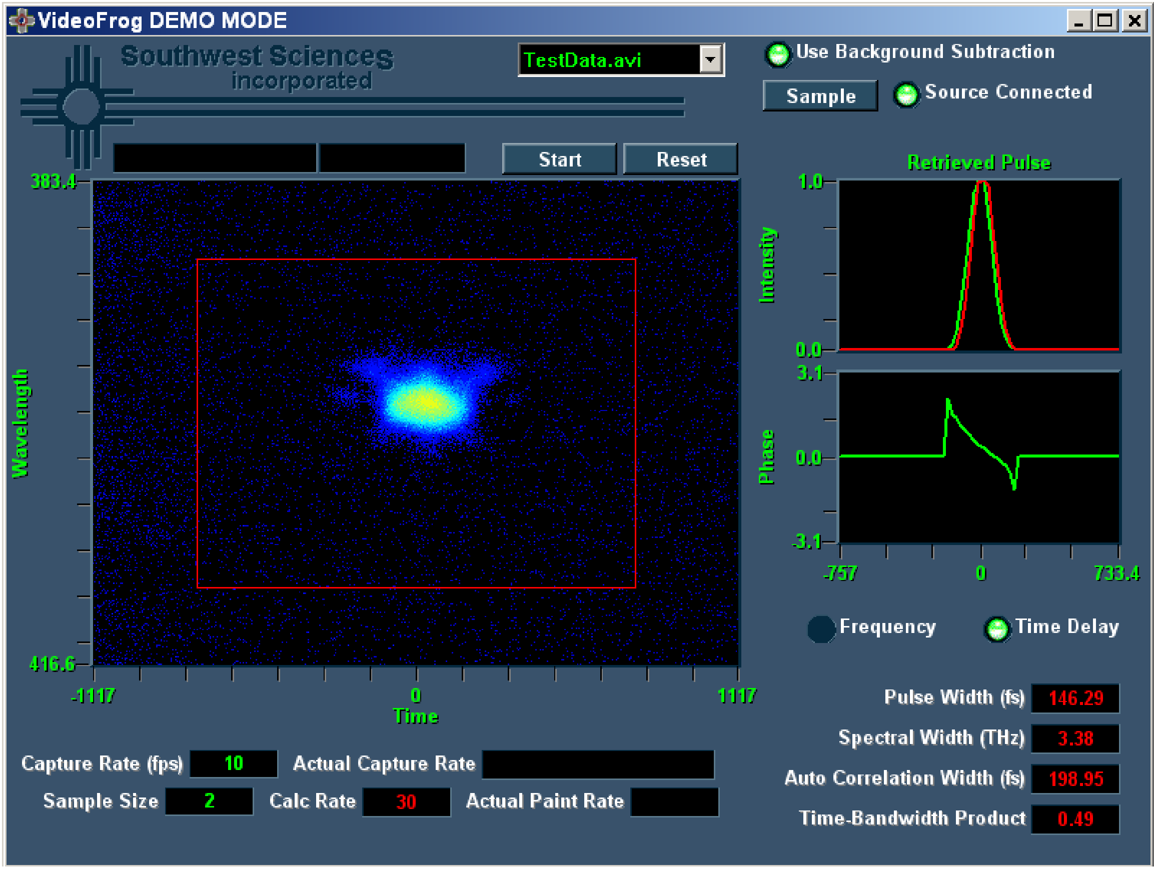

Figure 1.3. Screen capture of the FROG trace and reconstruction of pulses from the laser amplifier (TSA).

1.3. NUMERICAL SIMULATIONS

We have used computer simulations to calculate the pulse propagation in a self-focusing material. The numerical results complement the experimental results and provide insight into the mechanisms responsible for the measured effects. The propagation of ultrashort pulses is modeled using the nonlinear Schrodinger equation (NLSE). The equation is derived from Maxwell's equations by including the nonlinear polarization terms and applying some approximations (see Appendix A for the derivation). The NLSE describes the propagation of the complex envelope of the electric field. For a pulse propagating in the *z*-direction:

$$\frac{\partial A}{\partial z} = -i\frac{k_2}{2}\frac{\partial^2 A}{\partial u^2} + \frac{i}{2k_0}\nabla_T^2 A + i\frac{k_0}{n_0}\left(n_2|A|^2 + n_4|A|^4\right)A \tag{1.1}$$

where $\nabla_T^2 = \frac{\partial^2}{\partial x^2} + \frac{\partial^2}{\partial y^2}$ is the diffraction operator and $u = t - \frac{z}{v_g}$ is the time in a reference frame moving along with the pulse at the group velocity v_g. A is the complex envelope of the electric field, $k_0 = n_0\frac{\omega_0}{c}$, n_0 is the linear part of the refractive index of the medium, ω_0 is the carrier frequency of the pulse, c is the speed of light, k_2 is the coefficient for group velocity dispersion and n_2 and n_4 are the coefficients for third and fifth order nonlinearities, respectively. The intensity of the light is proportional to $|A|^2$.

The equation above describes how the field evolves with propagation distance. The first term on the right hand side accounts for group velocity dispersion, the second accounts for diffraction and the last term accounts for third and fifth order optical nonlinearities. It is computationally very expensive to numerically solve the equation in three spatial dimensions and time, so we have also used a time-averaged NLSE, where A_s is a time averaged field that depends only on the spatial coordinates:

$$\frac{\partial A_s}{\partial z} = \frac{i}{2k_0}\nabla_T^2 A_s + ik_0\left(n_2|A_s|^2 + n_4|A_s|^4\right)A_s \tag{1.2}$$

The NLSE is solved numerically using the Split-step Fourier method [15]. The propagation is solved in steps by splitting each step into the linear and nonlinear parts of the propagation. The linear part (diffraction) is solved by Fourier-transforming the equation to the frequency domain. The equation is then Fourier-transformed back to the time domain where the nonlinear step is calculated. The step size and number of pixels required for the simulation depends on the strength of the nonlinearity and the intensity of the light. The effect of the nonlinearities is that the beam will see index changes proportional to the intensity (n_2) and to the square of the intensity (n_4). If n_2 is positive, and n_4 negative, the interplay between diffraction and nonlinearities induces the formation of spatial solitons, or light filaments. The filaments can propagate for a distance much greater than the diffraction length with a constant diameter. In the simulations we have observed the beam to break up into multiple filaments, which then interact with their neighbors. The experimental results were compared with the numerical results and found to be in good agreement.

1.4. THESIS OUTLINE

The first half of this thesis describes the implementation of a novel holographic system to capture the propagation of femtosecond pulses. The holographic camera can reconstruct index and absorption changes inside the material with very fine spatial and temporal resolution. Chapter 2 is a theoretical analysis of recording and reconstructing holograms with femtosecond pulses. The chapter describes the origin of the nonlinear index changes, i.e., the Kerr effect and plasma formation. The use of on-axis holograms results in the appearance of a twin image, which introduces artifacts in the reconstructed field. We developed an algorithm to numerically remove the distortion due to the twin image. There are also issues that are unique to holography with ultrashort pulses, such as the geometry of the overlap of pump and probe pulses and the coupling between temporal and spatial resolution. In Chapter 3 we present results on pulse propagation through different materials captured with the holographic system. Dramatic differences were observed in the propagation of pulses in air, water, carbon disulfide and lithium niobate.

The second half focuses on the formation and interaction of spatial solitons in a self-focusing medium. In Chapter 4 we have investigated the mechanisms involved in the formation of solitons by observing the beam profile as a function of energy and propagation distance. We have discovered that the emission of conical waves plays a fundamental role in the formation of spatial solitons. Chapter 5 presents a study of the collective behavior of spatial solitons. We have observed the emergence of order as solitons appear on the beam profile followed by a transition to a chaotic state when the density of solitons becomes too high. When the solitons are generated in an unstable configuration they self-organize into an array with a larger period. The results in Chapters 4 and 5 are complemented by numerical simulations of the pulse propagation.

REFERENCES

[1] J. P. Gordon, Optics Letters **8**, 596 (1983).

[2] G. I. Stegeman and M. Segev, Science **286**, 1518 (1999).

[3] R. L. Fork, C. V. Shank, C. Hirlimann, et al., Optics Letters **8**, 1 (1983).

[4] D. J. Kane and R. Trebino, IEEE Journal of Quantum Electronics **29**, 571 (1993).

[5] Cordin Scientific Imaging, [http://www.cordin.com].

[6] Hamamatsu, [http://www.hamamatsu.com].

[7] N. Abramson, Applied Optics **22**, 215 (1983).

[8] Z. W. Liu, M. Centurion, G. Panotopoulos, et al., Optics Letters **27**, 22 (2002).

[9] Z. W. Liu, G. J. Steckman, and D. Psaltis, Applied Physics Letters **80**, 731 (2002).

[10] D. Gabor, Nature **161**, 777 (1948).

[11] H. Schroeder and S. L. Chin, Optics Communications **234**, 399 (2004).

[12] M. Fujimoto, S. Aoshima, M. Hosoda, et al., Optics Letters **24**, 850 (1999).

[13] M. Centurion, Y. Pu, and D. Psaltis, Physical Review Letters (2005).

[14] M. Centurion, Y. Pu, M. Tsang, et al., Physical Review A (2005).

[15] G. P. Agrawal, *Nonlinear fiber optics* (Academic Press, San Diego, 1995).